Finite Element Simulation of Cutting Temperature Distribution in Coated Tools During Turning Processes

Jingjie Zhang[1,2,3(✉)], Guanghui Fan[1,2], Liwei Zhang[4], Lili Fan[1,2], Guoqing Zhang[1,2], Xiangfei Meng[1,2], Yu Qi[1,2], and Guangchen Li[1,2]

[1] Faculty of Mechanical Engineering, Qilu University of Technology (Shandong Academy of Sciences), Jinan 250353, China
zjj@qlu.edu.cn

[2] Key Laboratory of Equipments Manufacturing and Intelligent Measurement and Control, China National Light Industry, Qilu University of Technology (Shandong Academy of Sciences), Jinan 250353, China

[3] School of Materials Science and Engineering, Shandong University, Jinan 250000, China

[4] School of Civil Engineering, Qingdao University of Technology, Qidao 266000, China

Abstract. The effect of cutting temperature on mechanism of cutting process has been a fundamental issue. Cutting tool temperature has significant influences on wear behavior of cutting tool, surface finish and surface integrity during the cutting process. Advanced coating materials are appropriate to deposit on the carbide substrate to enhance the tool performance and then prolong the tool life. This paper presents the cutting temperature of coated tool based on the cutting process simulation with finite element method (FEM) simulation by using Third Wave AdvantEdge software. The influences of coating materials and coating thickness on the temperature distribution in coated cutting tools were investigated. The simulated results showed that the temperature gradually increases in the tool-chip contact area. And the temperature rapidly decreases after the tool-chip separation point. TiAlN coating showed a better thermal barrier property than other coatings at the same conditions. The cutting tool temperature of TiN coated cutting tools with different coating thickness was also investigated with FEM. The temperature distribution at the tool rake face and substrate temperature were different for various coating thicknesses.

Keywords: cutting temperature · coated tools · coating material · coating thickness · finite element simulation

1 Introduction

In machinery manufacturing, although a variety of molding processes for different parts have developed, still more than 90% of the mechanical parts are made by cutting. In metal cutting, heat sources responsible for high temperature rise include plastic deformation

B. Wang et al. (Eds.): ICMTEL 2023, LNICST 535, pp. 319–328, 2024.
https://doi.org/10.1007/978-3-031-50580-5_28

in the shear zones and friction at the tool-chip interface and tool-workpiece interface. The generated heat mainly diffuses into four parts: chips, cutting tools, workpiece and environment.

Recent studies have shown a good correlation between tool temperature and tool life [1–4]. And the temperature has a great influence on the wear mechanism and performance of the tool. In metal cutting, cutting temperatures leads to chemical element diffusion and the oxidation [5, 6]. It will weaken tool strength and reduce the tool service life. In metal cutting, the distribution of temperature fields and heat dissipation are mainly dominated by the thermo-physical properties of tool and workpiece materials [7]. The tool coating has high hardness, temperature and oxidation resistance, and poor friction coefficient [8]. Compared with uncoated tools, coated tools can improve the cutting speed, tool life and cutting efficiency. Coating materials and the number of coating layers have effects on coated tool cutting temperature. In particular, the temperature plays an important role in cutting, so cutting temperature research and measurement has become the focus of the cutting experiment. Among the temperature research, the maximum temperature and the temperature distribution of the rake face is the key to temperature research. Generally, there are mainly two ways to measure the cutting temperature: contact and noncontact. Abukhshim [9] used the digital infrared pyrometer to measure the cutting temperature in turning experiments. The temperature profiles of the cutting tool is obtained by the finite element transient thermal analysis. The results shows that the temperature of the rake face increases with the cutting speed. The temperature variation beneath on the rake face of a cutting tool were analyzed by the Green's function approach. And the temperature variation on the rake face were obtained by a pyrometer consisting of two optical fibers and a fiber coupler during the milling process [10]. Saelzer [11] carried out orthogonal cutting experiments to investigate the contact behavior between the tool and the chip. In experiments, cutting temperature on the rake face of orthogonal cutting was directly measured by a two-color fiber pyrometer Fire III, built by the company En2Aix. The result shows that the temperature of the chip surface is independent of the cutting speed and the uncut thickness of the chip, but the cutting speed has a strong influence on rake face temperature. The temperature of the rake face increases with the cutting speed. In order to test the tool temperature distribution in the processing of machining titanium alloys and considered the fact that carbide inserts are easy to wear when machining titanium, Li [12] designed a cemented carbide tools embedded with thin film thermocouples, and made micro-grooves on the rake face near the tip through laser machining, and installed the thin film sensors in the micro-grooves. Besides, the modeling approach is used to predict the temperature on the rake face, MöHring [13] shown that the numerical iteration method to calculate the cutting temperature, and the new method takes the heat distribution for moving sources into account. In the high-speed milling process, the heat flux and temperature distribution on the tool-chip interface were analyzed by a three-dimensional inverse heat-transfer model [14].

In recent years, the technology of FEM has been widely used for the simulation of metal cutting. In this paper, the commercial Third Wave AdvantEdge software was employed to develop a coupled thermo-mechanical finite element model for cutting temperature simulation of monolayer coating cemented carbide tools in the orthogonal metal cutting process. The cutting process is simulated from the initial to the steady-state

phase. The effects of main factors of coating materials and coating thickness on cutting temperature distribution are investigated.

2 Finite Element Modeling of Orthogonal Cutting Process

Komanduri [15] reported that the heat sources in metal cutting responsible for high temperature rise include (1) heat dissipation due to plastic deformation in the shear zones and (2) friction heat generated at the tool-chip and tool-workpiece interfaces. Figure 1 shows these main heat sources generated in the cutting process.

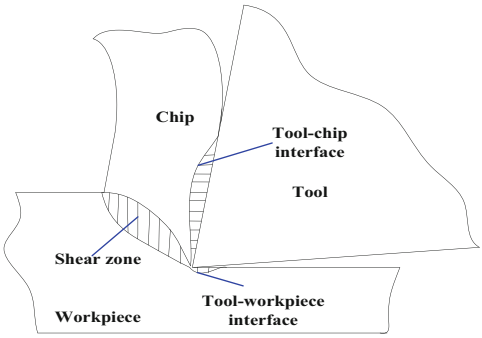

Fig. 1. Principal of heat sources in metal machining

2.1 Boundary Conditions

As shown in Fig. 2, the boundary condition of the FEM is set as follows. (1) Machining is performed at ambient temperature, which is equal to the room temperature (Tr = 20 °C). (2) For the noncontact surfaces of the tool and workpiece, heat loss due to heat convection ($h_a = 20\ W/m^2{}^\circ C$) and thermal radiation to the environment was considered.

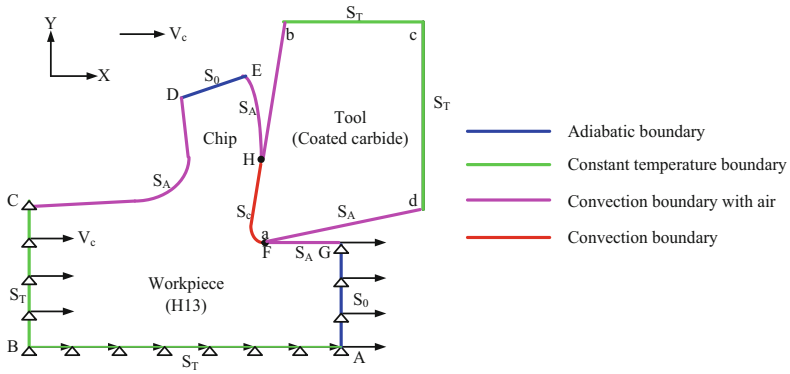

Fig. 2. Boundary conditions in metal cutting modeling

The thermal boundary conditions are summarized below. (1) ST is a constant temperature boundary, and the temperature is room temperature (Tr = 20 °C). (2) SC is convection boundary with chip. This boundary is the tool-chip interface, which has frictional heat. (3) SA is convection boundary with air (ha = 20 W/m^2 °C). (4) S0 is an adiabatic boundary. The boundaries including ST, SC, SA, and S0 are detailed in Fig. 2.

2.2 Graphical Representation of the Simulation Model

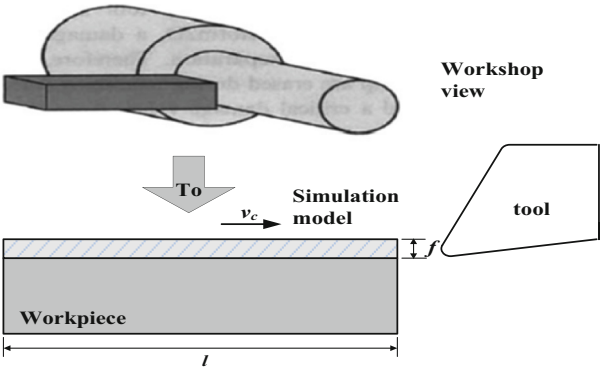

(a) Graphical representation of cutting process

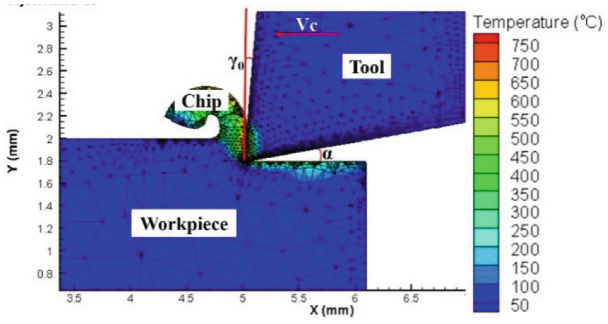

(b) FEM simulation model

Fig. 3. Graphical representation of FEM simulation model

The simplification of the cutting process and the construction of the simulation model are shown in the Fig. 3. Where Vc is the cutting speed; f is the feed rate; γ0 is the rake angle; α is the relief angle.

The tool model consists of an adequate number of node planar heat-transfer elements, because heat transfer analysis is carried out on it.

2.3 Cutting Conditions

The orthogonal cutting processes without coolant were simulated. The workpiece material used in the simulation was a hardened steel of H13 with the ultimate tensile UST = 1882 MPa. The cutting speeds were 300 m/min and 500 m/min, respectively. Undeformed chip thickness was fixed at 0.2 mm, and the width of cut was 0.25 mm. Machining is performed at ambient temperature, which is equal to the room temperature (Tr = 20 °C).

3 Simulated Results and Discussion

The effect of coating materials and coating thickness of coated tools on cutting temperature distribution is investigated in the FEM simulation. In addition, the temperature distribution on the tool rake face and in the tool body is simulated and analyzed.

3.1 Simulation of Cutting Temperature of Different Coating Material

Three kinds of monolayer coated tools with TiN, TiC and TiAlN coating, respectively, were employed in this investigation. Their substrate bulk materials were cemented carbide. The coating thickness of these three kind tools was 2 μm.

As shown in Fig. 4, the tool-chip interface is the main area of the temperature distribution. Therefore, the tool-chip interface temperature is important for the coated tools investigated. The temperature distribution perpendicular to the cutting tool rake face is then investigated to study the heat conduction in the cutting tools with different coating layers.

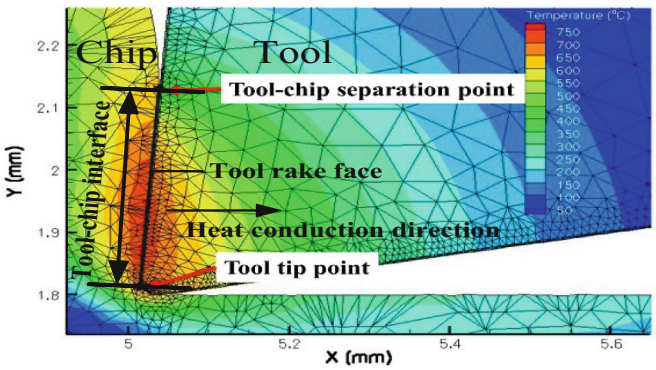

Fig. 4. Schematic of cutting temperature distribution

3.1.1 Temperature Distribution on Tool Rake Face

The temperature of the tool-chip interface are obtained by the FEM. The temperature results obtained for the different coatings are shown in Fig. 5. As shown in Fig. 5, the

temperature along the tool-chip interface increases with distance from the tool tip. After the tool-chip separation point, the temperature shows a decreasing trend. Because of the rake face temperatures are mainly depend on the secondary deformation friction heat. The friction between the tool and chip disappears after the tool-chip separation point, which it will cause the temperature decrease.

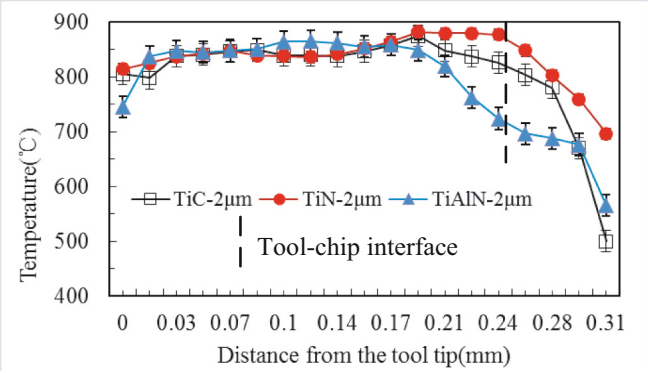

Fig. 5. Cutting temperature distribution on rake face for TiN, TiC and TiAlN coated tools

Figure 5 shows that the cutting temperatures on rake face of TiC, TiN and TiAlN coated tools are different. The rake face temperature of TiN and TiC coated tools are higher than that of TiAlN coated tool at the same position on rake face. The rake face temperature of TiC coated tool is the highest. The average temperature of rake face and tool-chip interface for these three-coated tools was shown in Table 1. The average rake face temperature and the average tool-chip interface temperature of these three kinds have a relationship as follow: TiAlN<TiC<TiN. This difference is from the friction coefficients for different material pairs among TiAlN/workpiece, TiN/workpiece and TiC/workpiece, respectively. The frictional coefficient between the coated tools and the H13 are as follows: TiAlN/H13(0.3)<TiN/H13(0.4)<TiC/H13 [16, 17]. Higher frictional coefficient introduces the higher frictional force on the tool-chip interface, and then induces the higher frictional heat. It indicates that the TiAlN coating has better anti-friction performance than other coatings. It can reduce the frictional force and frictional heat in the cutting process.

Table 1. The average temperature (°C) of rake face and tool-chip interface for three coated tools

Average Temperature	TiC-2 μm	TiN-2 μm	TiAlN-2 μm
Rake face	807.64	835.15	792.89
Tool-chip interface	839.28	850.68	829.18

3.1.2 Temperature Distribution Perpendicular to Rake Face

Temperature distributions in the tool body of these three kinds of coated tools are displayed in Fig. 6. As shown in Fig. 6, the temperature perpendicular to rake face for TiC, TiN and TiAlN coated tool decrease with the distance from rake face. At the same position, the temperature for TiAlN coated tool is lower than those of TiC and TiN coated tools. This difference can illustrate the heat-conducting property of coating material and the heat conduction property between coating and substrate.

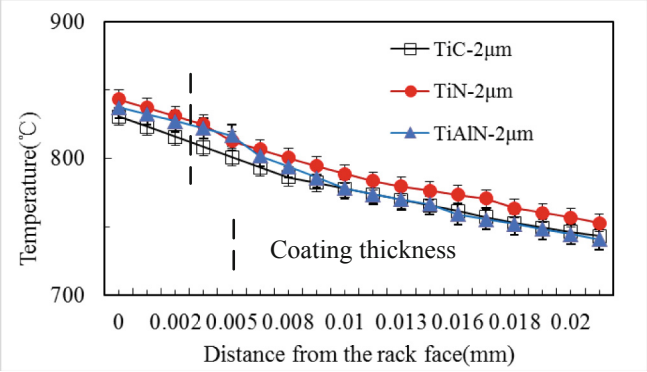

Fig. 6. Temperature distribution in tool body of TiN, TiC and TiAlN coated tool

3.2 Cutting Temperature of Different Coating Thickness for TiN Coated Tool

In this section, TiN coated tools (substrate of Cemented Carbide) with different coating thicknesses (1, 2, 5,10 μm) are selected to explore the influence of coating thickness on cutting temperature. Among of them, TiN-1 μm (coating thickness of 1 μm), TiN-2 μm (coating thickness of 2 μm), TiN-5 μm (coating thickness of 5 μm) and TiN-10 μm (coating thickness of 10 μm). The temperature distribution on the rake face and in the tool body of TiN coated tool for different thickness is investigated for researching the effect of coating thickness.

The results obtained from four kinds of TiN coated tools are marked in Fig. 7 and Fig. 8. As shown in Fig. 7, the temperature gradually increases in the tool-chip contact area. And the temperature rapidly decreases after the tool-chip separation point. Rake face temperature of four kinds of TiN coated tools showed the same trend, just the value of rake face temperature is different. The temperature distributions in four kinds of TiN cutting substrate all decrease with the distance from the tool rake face. Similarly, the trend of temperature is the same for all coated tools. The rake face temperature and the substrate temperature versus different thickness TiN coated tool have relationships as follows: TiN-1μm≈TiN-2 μm<TiN-10 μm<TiN-5 μm. This can illustrate that the coating effect of 1 μm and 2 μm coating thickness TiN coated tools is not obvious. TiN-5 μm has the highest temperature in the four kinds of TiN coated tools. When coating thickness keeps on increasing, the temperature of the TiN-10 μm decreased. It can be

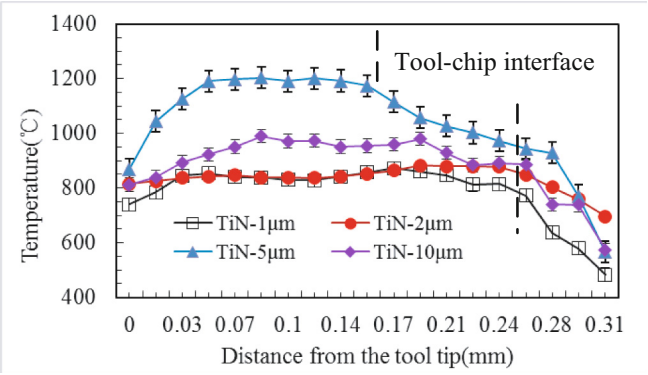

Fig. 7. Cutting temperature distribution on rake face of TiN coated tools versus different coating thickness

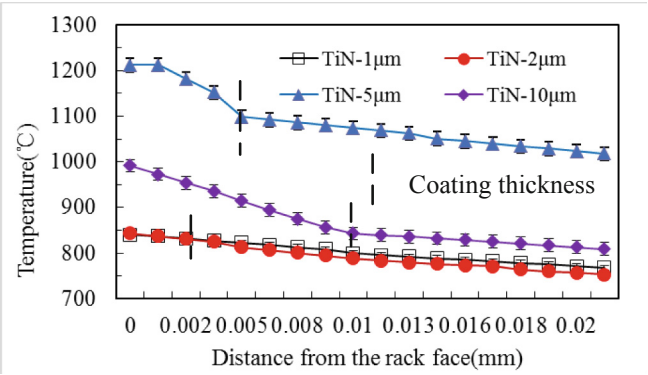

Fig. 8. Temperature distribution in the tool body versus different coating thickness

considered that the thickness is 5 μm, heat insulation effect of TiN coating did not play, only the coating thickness to a certain degree such as 10 μm, heat insulation effect of the TiN coating is played.

Therefore, for the same kind of coated tools, the cutting temperature for the thick thickness of coating is not lower than the thin thickness of coating. It is either related to the structure of the coating, or related to the coating material and workpiece material.

4 Conclusions

In this paper, the heat conduction of coated tools was investigated through the FEM. The coating material and coating thickness of the coated tools are analyzed for the heat conduction during the cutting process. The main conclusions are as follows:

(1) At the rake face, the temperature gradually increases in the tool-chip contact area. And the temperature rapidly decreases after the tool-chip separation point.

(2) As the distance from rake face increases, the cutting temperature of the coated tools gradually decreases.
(3) At the same conditions, TiN and TiC coating material have a worse thermal property than TiAlN coating material. Under the same coating material, 1 and 2 μm thickness presents better thermal properties than TiN-5μm and TiN-10 μm coated tools.

Acknowledgments. This work is supported by the National Natural Science Foundation of China (Grant Nos. 51905286, 52075276), and the Science, education and industry integration project of Qilu University of Technology (Grant No. 2022PY006).

References

1. Soler, D., Aristimuo, P.X., Garay, A., Arrazola, P.J., Klocke, F., Veselovac, D., et al.: Finding correlations between tool life and fundamental dry cutting tests in finishing turning of steel. Procedia Eng. **132**, 615–623 (2015)
2. Asha, P.B., Rao, C., Kiran, R., Kumar, D.: Effect of machining parameters on cutting tool temperature and tool life while turning EN24 and HCHCr grade alloy steel. Mater. Today Proc. **5**(5), 11819–11826 (2018)
3. Hao, G., Liu, Z.: Thermal contact resistance enhancement with aluminum oxide layer generated on TiAlN-coated tool and its effect on cutting performance for H13 hardened steel. Surf. Coat. Technol. **385**(C), 125436 (2020)
4. Kovac, P., Gostimirovic, M., Rodic, D., Savkovic, B.: Using the temperature method for the prediction of tool life in sustainable production. Measurement **133**, 320–327 (2019)
5. Shalaby, M.A., Veldhuis, S.C.: Wear and tribological performance of different ceramic tools in dry high speed machining of Ni-Co-Cr precipitation hardenable aerospace superalloy. Tribol. Trans. **62**(1), 62–77 (2018)
6. Wang, B., Li, A., Liu, G.: Cutting performance and wear mechanisms of TiAlN PVD-coated cemented carbide tool in high speed turning of Ti-5Al-2Sn-2Zr-4Mo-4Cr alloy. J. Mech. Sci. Technol. **34**(7), 2997–3006 (2020)
7. Grzesik, W., Nieslony, P.: Physics based modelling of interface temperatures in machining with multilayer coated tools at moderate cutting speeds. Int. J. Mach. Tools Manuf **44**(9), 889–901 (2004)
8. Aihua, L., Jianxin, D., Haibing, C., Yangyang, C., Jun, Z.: Friction and wear properties of TiN, TiAlN, AlTiN and CrAlN PVD nitride coatings. Int. J. Refract Metal Hard Mater. **31**, 82–88 (2012)
9. Abukhshim, N.A., Mativenga, P.T., Sheikh, M.A.: Investigation of heat partition in high speed turning of high strength alloy steel. Int. J. Mach. Tools Manuf **45**(15), 1687–1695 (2005)
10. Sato, M., Tamura, N., Tanaka, H.: Temperature variation in the cutting tool in end milling. J. Manuf. Sci. Eng. **133**(2), 021005 (2011)
11. Saelzer, J., Berger, S., Iovkov, I., Zabel, A., Biermann, D.: In-situ measurement of rake face temperatures in orthogonal cutting. CIRP Ann. Manuf. Technol. **69**(1), 61–64 (2020)
12. Li, J., Tao, B., Huang, S., Yin, Z.: Built-in thin film thermocouples in surface textures of cemented carbide tools for cutting temperature measurement. Sens. Actuators A **279**, 663–670 (2018)
13. MöHring, H.C., Kushner, V., Storchak, M., Stehle, T.: Temperature calculation in cutting zones. CIRP Ann. Manuf. Technol. **67**(1), 61–64 (2018)

14. Ming, C., Sun, F., Wang, H., Yuan, R., Qu, Z., Zhang, S.: Experimental research on the dynamic characteristics of the cutting temperature in the process of high-speed milling. J. Mater. Process. Technol. **138**(1), 468–471 (2003)
15. Komanduri, R., Zhen, B.H.: Thermal modeling of the metal cutting process-Part II: temperature rise distribution due to frictional heat source at the tool–chip interface. Int. J. Mech. Sci. **43**(1), 57–88 (2001)
16. Rech, J.: Influence of cutting tool coatings on the tribological phenomena at the tool–chip interface in orthogonal dry turning. Surf. Coat. Technol. **200**(16), 5132–5139 (2006)
17. Zhang, S.: Prediction and measurement of cutting temperature for coated tools. Shandong University (2009)